



A NONLINEAR MODEL OF AEROELASTIC BEHAVIOUR OF ROTOR BLADES IN FORWARD FLIGHT

By

A. Rosen and O. Rand

Department of Aeronautical Engineering  
Technion - Israel Institute of Technology  
Haifa 32000, Israel

**TENTH EUROPEAN ROTORCRAFT FORUM**  
**AUGUST 28 – 31, 1984 – THE HAGUE, THE NETHERLANDS**

# A Nonlinear Model of Aeroelastic Behaviour of Rotor Blades in Forward Flight

A. Rosen and O. Rand

Department of Aeronautical Engineering  
Technion - Israel Institute of Technology  
Haifa 32000, Israel

## Abstract

The paper presents a nonlinear model of the aeroelastic behaviour of rotor blades. This model is based on two sub-models. The first one is a nonlinear structural/dynamic model while the second is a prescribed-wake unsteady aerodynamic model. These two sub-models have been described previously in detail and therefore are described here only briefly. The paper concentrates on the method of combining these two sub-models. Since these sub-models are nonlinear and the steady state is of nonlinear periodic nature, there are certain difficulties in obtaining the final complete aeroelastic response. The paper presents the iterative interactive approach which has been developed and discusses the different problems associated with this model. Two examples will be presented where the theoretical results are compared with existing experimental results. It will be shown that good agreement is obtained in most of the cases.

## 1. Introduction

Recently [1] a new general model of helicopter blade dynamics has been presented. From a structural point of view the blade is modeled as a curved rod while nonlinear effects are included. The nonlinear derivation is restricted to the case of small strains and moderate elastic rotations, while no further simplifying assumptions are adopted. There is a special treatment of the blade root which enables the accurate modeling of different kinds of rotors including: articulated rotors, hingeless rotors, elastomeric bearings and any other kind of attachment of the blade to the rotor hub. As explained in [1] the inertia loads are also treated in an accurate manner while all the nonlinear effects due to the hub motions, motions of the blade root relative to the hub, and elastic deformations, are taken into account. Any planar geometry of the blade and any spanwise distribution of the structural and inertia (mass) properties are allowed.

The main purpose of [1] has been the presentation of an accurate structural and dynamic model of the blade. Only a very simple model for calculating the aerodynamic loads has been used there. On the other hand, another recent paper [2] concentrated on presenting a relatively efficient and accurate model of calculating the blade's aerodynamic loads in forward flight. This is a general model which contains different new features compared with other models which have been reported in the literature. The model itself is a prescribed-wake model which includes unsteady aerodynamic effects.

The present paper will present how the structural/dynamic model of the blade [1] is combined with the aerodynamic model of [2] to yield a complete model for the nonlinear aeroelastic behaviour of rotor blades in forward flight. The combination of these two models presents different problems which will be discussed throughout the paper. In order to show the capabilities of the model, a comparison between its results and experimental results which has been previously reported, will be presented.

There are a few other different models of the aeroelastic behaviour of blades, which are in use at different places. It is beyond the scope of this paper to present a survey of all these models. The interested reader is referred to [3]. A recent successful well known example is a model which had been developed by W. Johnson [4,5]. The present model presents an effort to avoid many of the limiting assumptions which have been adopted while developing the previous models. On the other hand another effort has been aimed at avoiding the necessity of enormous computer resources.

## 2. Description of the Model

In what follows the complete model will be described. The structural/dynamic model has been previously described [1] and the same applies to the aerodynamic model [2]. Therefore, only details which are necessary for the completeness of the paper will be presented, concerning these two sub-models. The paper will concentrate on the method by which these two sub-models are combined in order to yield a complete nonlinear aeroelastic model.

### 2.1 The Structural Contributions and the Inertia Loads

The model which describes the structural behaviour of the blade and the inertia loads is presented in detail in [6]. This model has been described more briefly in [1]. The structural model itself is described in more detail in [7] while [8] concentrates on the blade dynamics and inertia contributions.

The helicopter hub may have any combination of linear and angular motions including both linear and angular accelerations. The blade is attached to the hub as described by Fig. 1.  $f_x$ ,  $f_y$ , and  $f_z$  are the linear displacements of the blade root (relative to the shaft), while  $\beta$ ,  $\zeta$  and  $\theta$  are the root rotations (flapping, lead-lag and pitch angles, respectively). Finite values of these linear displacements and rotations are assumed and there are no restrictions on their magnitude. Since the angles are finite, the sequence of the three hinges is important. It is fairly easy to replace the sequence of Fig. 1 by any other sequence. The behaviour of  $f_x$ ,  $f_y$ ,  $f_z$ ,  $\beta$ ,  $\zeta$  and  $\theta$  is a function of the type of rotor which is considered and the kind of attachment of the blade to the hub (hingless, articulated, elastomeric bearings etc.).

The blade system of coordinates ( $x_B$ ,  $y_B$ ,  $z_B$ ), which is defined by the linear displacements and angular rotations at the blade root (see Fig. 1), is used in order to describe the elastic axis of the blade before and after the deformation.  $x$  is a curved coordinate line along the blade which is equal to zero at the blade root and is equal to  $L$  at the blade tip, while  $L$  is the blade length.  $x_B(\alpha)$  and  $y_B(\alpha)$  define the shape of the blade before the deformation (see Fig. 2) where  $\alpha$  is a nondimensional curved

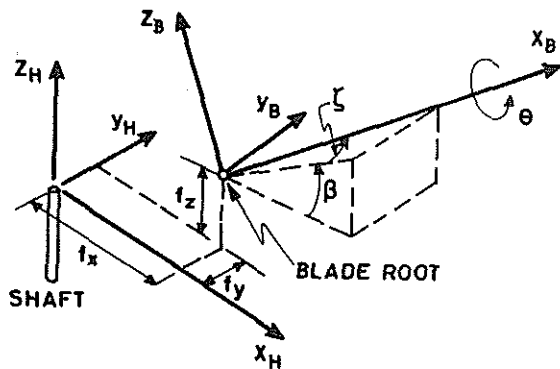


Fig. 1. The root motions.

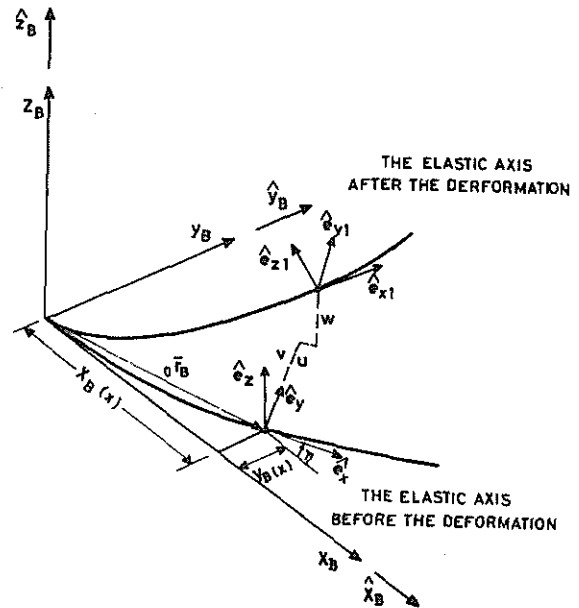


Fig. 2. The elastic axis of the blade before and after the deformation.

coordinate along the blade axis ( $x/L$ ). The present model is restricted to the case of planar curvature. If Bernoulli-Euler hypothesis is adopted [1,6,7] then the location of each material point of the blade, after the deformation, is defined by the displacement of the elastic axis. This displacement is described by its components:  $u$  (axial),  $v$  (edgewise) and  $w$  (beamwise) (see Fig. 2). In the case of a straight blade  $u, v, w$  are in the directions of the coordinate lines  $x_B, y_B, z_B$  respectively. In addition, there is also a rotation  $\phi$  of the cross section about the elastic axis. In the derivation of the structural model the assumption of small strains and moderate elastic rotations is adopted. In addition, it is also assumed that the warping displacements are small compared with typical cross sectional dimensions. No further assumptions are used besides these assumptions. All the nonlinear structural coupling effects are taken into account in an accurate manner.

Based on the above description the unknowns are  $\beta, \zeta, \theta, u, v, w$  and  $\phi$ . It should be remembered that at a trimmed forward flight all the unknowns are periodic functions where the basic period is the time required for one revolution of the rotor. In addition  $u, v$  and  $w$  are also functions of the nondimensional spanwise coordinate  $\alpha$ . It is convenient to replace  $u$  (as unknown) by  $P$ , the axial components of the cross sectional resultant force.

The equations are solved by Galerkin method where the unknowns are described by the following series:

$$\overset{\circ}{v} = v/L = \sum_{j=1}^N v_j FV_j \quad (1-a)$$

$$\dot{w} = w/L = \sum_{k=1}^{N_w} w_k F W_k \quad (1-b)$$

$$\dot{\phi} = \sum_{l=1}^{N_\phi} \phi_l F \phi_l \quad (1-c)$$

$$\dot{p} = \sum_{m=1}^{N_p} p_m F P_m \quad (1-d)$$

$FV_j$ ,  $FW_k$ ,  $F\phi_l$  and  $FP_m$  are predetermined shape functions. The unknowns become the coefficients  $v_j$ ,  $w_k$ ,  $\phi_l$  and  $p_m$ . These coefficients are in general functions of time. In the case of trimmed forward flight they are periodic functions.

The inertia loads are dealt with in an accurate manner [1,6,8]. All the nonlinear effects are taken into account while the assumption of small strains and moderate elastic rotations is not applied while calculating these loads.

If the aerodynamic loads which act along the blade are known, then integration of the equations of motion [1,6] yields the blade motion at any moment. This means that  $\beta$ ,  $\zeta$ ,  $\theta$ ,  $v_j$ ,  $w_k$ ,  $\phi_l$  and  $p_m$  become known functions of time.

In order to calculate the aerodynamic loads it is necessary to know the components of the blade velocity (relative to an inertial system). The nondimensional component of this velocity which is normal to the blade surface is denoted  $\tilde{w}$  (the dimensional velocity is divided by the tip velocity due to the rotor rotation -  $\Omega R$ ) and is given by:

$$\tilde{w} = A + B\xi \quad (2)$$

$\xi$  is a nondimensional chordwise coordinate which is equal to -1 at the leading edge and 1 at the trailing edge.  $A$  and  $B$  are nondimensional coefficients which are functions of the spanwise coordinate  $\alpha$  and time. In the case of a trimmed forward flight  $A$  and  $B$  are periodic function. Since the blade rotates at a constant angular velocity it is convenient to replace the physical time by the blade azimuthal location  $\theta_k$  ( $\theta_k$  is equal to zero when the blade is above the tail). It is clear that  $A$  and  $B$  are explicit functions of all the coefficients  $v_j$ ,  $w_k$ ,  $\phi_l$  and  $p_m$ , the displacements and rotations at the root, and the hub linear and angular motions.

While  $\tilde{w}$  is the normal component of the blade velocity,  $\tilde{U}$  is the nondimensional tangential component which is perpendicular to  $\tilde{w}$ . The main contributions to  $\tilde{U}$  are the rotor rotation and the fuselage linear velocity. Since helicopter blades usually have high aspect ratio, chordwise variations of  $\tilde{U}$  are negligible.  $\tilde{U}$ , like  $\tilde{w}$ , is also easily calculated if the periodic behaviour of all the unknowns has been obtained.

## 2.2 The Aerodynamic Model

The aerodynamic model has been described in detail in [2,9]. This is a prescribed-wake unsteady model. The blade is divided into  $m$  segments. It is assumed that there is a constant total bound circulation along each segment where changes in the circulation occur only between segments. Because of the periodic nature of the phenomenon (in the case of trimmed flight) the non-dimensional total bound circulation of the  $j$ th element is described as follows:

$$\tilde{\Gamma}_B(j, \theta_k) = \sum_{p=1}^q \Gamma S(j, p) \sin p \theta_k + \sum_{p=0}^q \Gamma C(j, p) \cos p \theta_k \quad (3)$$

$q$  is the number of sine and cosine terms. The unknowns are the coefficients  $\Gamma S(j, p)$  and  $\Gamma C(j, p)$ . If the condition of non-penetration of the flow through the blade surface is applied at different control cross sections along the blade, then the following system of equations is obtained.

$$[C]\{\Gamma\} = \{d\} \quad (4)$$

$[C]$  is not necessarily a square matrix and therefore an overdetermined system of equations is obtained. This system is solved by applying least-squares method [9].  $\{\Gamma\}$  is the vector of unknowns and is composed of all the coefficients  $\Gamma S$  and  $\Gamma C$  of all the segments.  $[C]$  is a matrix which includes the influence coefficients of all the wake elements. This matrix is a function of the rotor properties, flight conditions, the average induced velocity over the disc ( $v_{iav}$ ), and the disc angle of attack relative to the free stream velocity,  $\alpha_D$ . The vector  $\{d\}$  is a function of  $A$  and  $B$  (see Eq. (2)) at the control cross sections.

It should be pointed out that the most time consuming stage of the aerodynamic calculations is the computation of the matrix  $[C]$ .

One of the basic simplifying assumptions which is used in the aerodynamic derivation is the assumption that the chordwise variation of the induced velocity may be neglected and instead an average representative cross sectional value may be used. This nondimensional induced velocity (the dimensional value is divided by  $\Omega R$ ) is denoted  $\lambda_0$  and is a function of the spanwise location of the cross section and the blade azimuthal location  $\theta_k$ .  $\lambda_0$  is obtained directly from the cross sectional total bound circulation, namely, the coefficients  $\Gamma S$  and  $\Gamma C$ . If  $\lambda_0$  is known, then the cross section lift ( $L_A$ ) and moment ( $M_A$ ), per unit length, are given by the following equations:

$$L_A / \frac{1}{2} \rho \Omega^2 R^3 = - 2\pi \tilde{U} \frac{b}{R} (2A + 2\lambda_0 + B) - 2\pi \left(\frac{b}{R}\right)^2 \left[ 3 \frac{\partial A}{\partial \theta_k} + 3 \frac{\partial \lambda_0}{\partial \theta_k} + \frac{\partial B}{\partial \theta_k} \right] \quad (5-a)$$

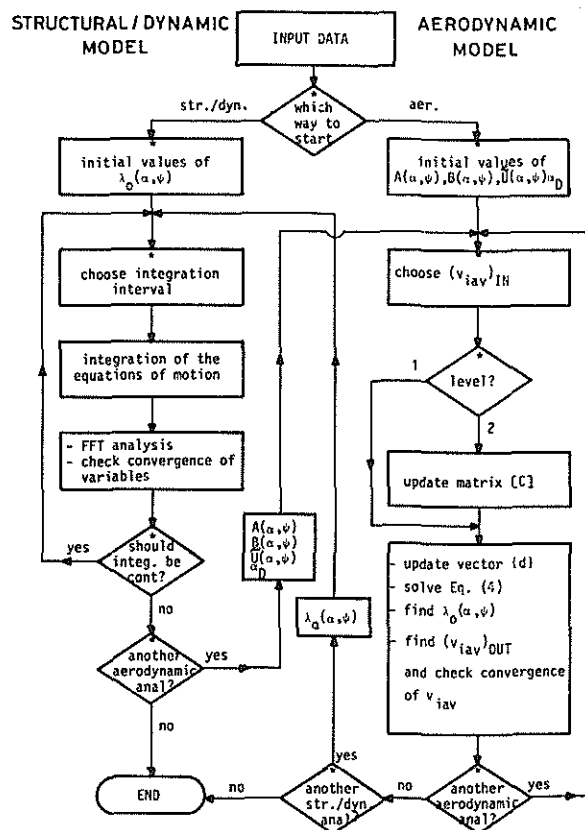
$$M_A / \frac{1}{2} \rho \Omega^2 R^4 = - 2\pi \tilde{U} \left(\frac{b}{R}\right)^2 (A + \lambda_0) + \pi \left(\frac{b}{R}\right)^3 \left( \frac{\partial A}{\partial \theta_k} + \frac{\partial \lambda_0}{\partial \theta_k} \right) + \frac{3}{4} \pi \left(\frac{b}{R}\right)^3 \frac{\partial B}{\partial \theta_k} \quad (5-b)$$

$b$  is half chord of the blade,  $\rho$  is the air mass density and  $\Omega$  the rotor angular velocity.

As indicated before, the aerodynamic model has been described very briefly while detailed description is given elsewhere [2,9]. But it is important to indicate that this model is basically nonlinear since the matrix  $[C]$  is a function of  $v_{iav}$ .  $v_{iav}$  is a weighted average of all the  $\lambda_0$  which are obtained by solving Eq. (4). Therefore the solution procedure includes an initial guess of  $v_{iav}$  which should be verified at the end of the calculation. If the value of  $v_{iav}$  which is obtained at the end of the calculation does not agree with the initial guess, then another value is assumed (this can be the new result or any value between the initial guess and the result) and the whole calculation procedure is repeated again.

### 2.3 The Complete Aeroelastic Behaviour

The structural/dynamic model of the blade and the aerodynamic model are highly coupled. Since this coupling is complicated and since each of these two models is nonlinear by itself, it will be too complicated to try and update both models simultaneously. Therefore, it has been decided that at any stage only one of the two will be updated while the other one will not be changed. Based on this strategy the solution procedure is described below and in Fig. 3.



\* indicate operator decision in the case of interactive mode

Fig. 3. Flow chart of the complete aeroelastic model.

At the beginning of the solution procedure, the input data is read and stored. This input data includes the geometric, structural, mass and aerodynamic properties of the rotor. In addition details which are necessary for the solution are also read which include for example: The different shape functions of Eqs. (1-a-d), details about the division into segments for the aerodynamic analysis, convergence criteria, etc. The solution procedure is started either with the structural/dynamic model or with the aerodynamic model. If it starts with the structural/dynamic model then an initial guess of  $\lambda_0$  is used. It should be remembered that in general  $\lambda_0$  is a function of  $\alpha$  and  $\psi$ . The simplest choice is that of a uniform  $\lambda_0$  which can be obtained by using elementary momentum/blade-element theory. In order to save computation time and accelerate the solution procedure it is also possible to use different models of non-uniform induced velocity distributions [10]. These distributions are obtained from simple analytic expressions and therefore are easy to apply. Now, integration of the equations of motion is started. In order to start the procedure a complete set of initial conditions is needed. This set includes all the unknowns and their first derivatives with respect to time. It is possible to take all the initial values equal to zero, but again in order to save computation time it is possible to begin from values which are obtained from simplified models of blade dynamics. The integration is carried out until convergence of the blade response is obtained. During the integration procedure the distribution of the aerodynamic loads along the blade is calculated by using Eqs. (5-a,b), where  $\lambda_0$  is the initial guess. It should be remembered that the phenomenon is periodic and therefore the convergence is also to a periodic solution. In order to obtain a measure of the convergence of this periodic solution, a Fast Fourier Transform is used in order to obtain a Fourier-Series description of the unknowns. Convergence of these coefficients indicates convergence to the periodic solution.

In Figs. 4 and 5 a simple example, which presents the technique, is shown. The case is that of a uniform blade with zero offset which is free to rotate about its flapping hinge. All the other motions and deformations are neglected. The advance ratio of the rotor is  $\mu=0.175$  and the shaft angle of attack is zero. The rotational speed is  $\Omega=150$  rad/sec while the disc radius is  $R=1.52$  m and the chord  $0.122$  m. The mass per unit length of the blade equals  $0.535$  kg/m and the air mass density is  $1.23$  kg/m<sup>3</sup>. The cross sectional lift curve slope equals  $5.9$  1/rad while the pitch angle (constant along the blade) is  $8^\circ$ . A uniform induced velocity is assumed which is equal to  $\lambda_0=0.04$ . The present structural/dynamic model has been used in order to calculate the blade flapping. In the calculations three different sets of initial conditions have been used and are indicated in the figures. The flapping response of the blade, in these three cases, is shown in Fig. 4. It can be seen that in all the cases the blade rapidly approaches the steady state periodic response. The periodic response can be represented by the following Fourier series.

$$\beta = a_0 + \sum_{n=1}^N \beta (a_n \cos n\theta_k + b_n \sin n\theta_k) \quad (6)$$

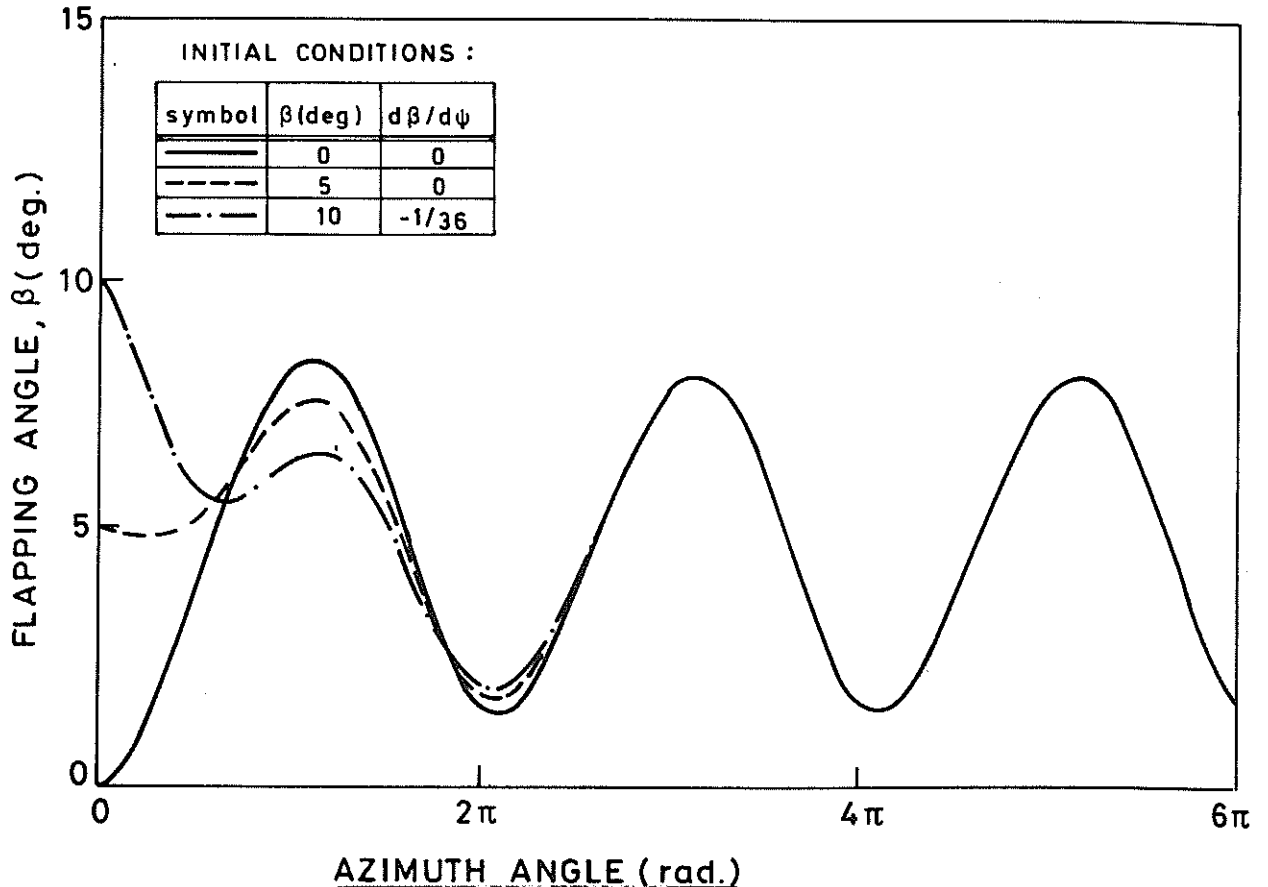


Fig. 4. Results of the integration for a simple case of uniform inflow.

After the first revolution, at the end of any azimuthal shift of  $\pi/2$  radians, an FFT of the flapping response (along the last  $2\pi$  radians) is performed. The coefficients  $a_0$ ,  $a_1$ ,  $b_1$  which are obtained from this FFT analysis are presented in Fig. 5. By looking at these results the convergence to the steady-state periodic solution is easily determined. It can be seen that  $a_0$  and  $a_1$  converge after only 1.75 revolutions, while  $b_1$  converges after 2.5 revolutions. It is clear that the Fourier analysis of the time response is a very useful tool in assessing the convergence to a steady state periodic solution.

As an output of the structural/dynamics model, the velocity at the aerodynamic control cross sections ( $\vec{U}, A, B$ ) and the blade motions relative to the hub (which have an influence on the disc angle of attack) are obtained. With this information the aerodynamic model is updated. There are two levels of updating this model. The first level includes only the updating of the vector  $\{d\}$  of Eq. (4). As already indicated, this vector is a relatively simple explicit function of  $A$ ,  $B$  and their derivatives with respect to the azimuthal location of the blade. The second level includes updating of the matrix  $[C]$  and is a much more complicated and time consuming level. It is necessary to update  $[C]$  only if the disc angle of attack has been changed

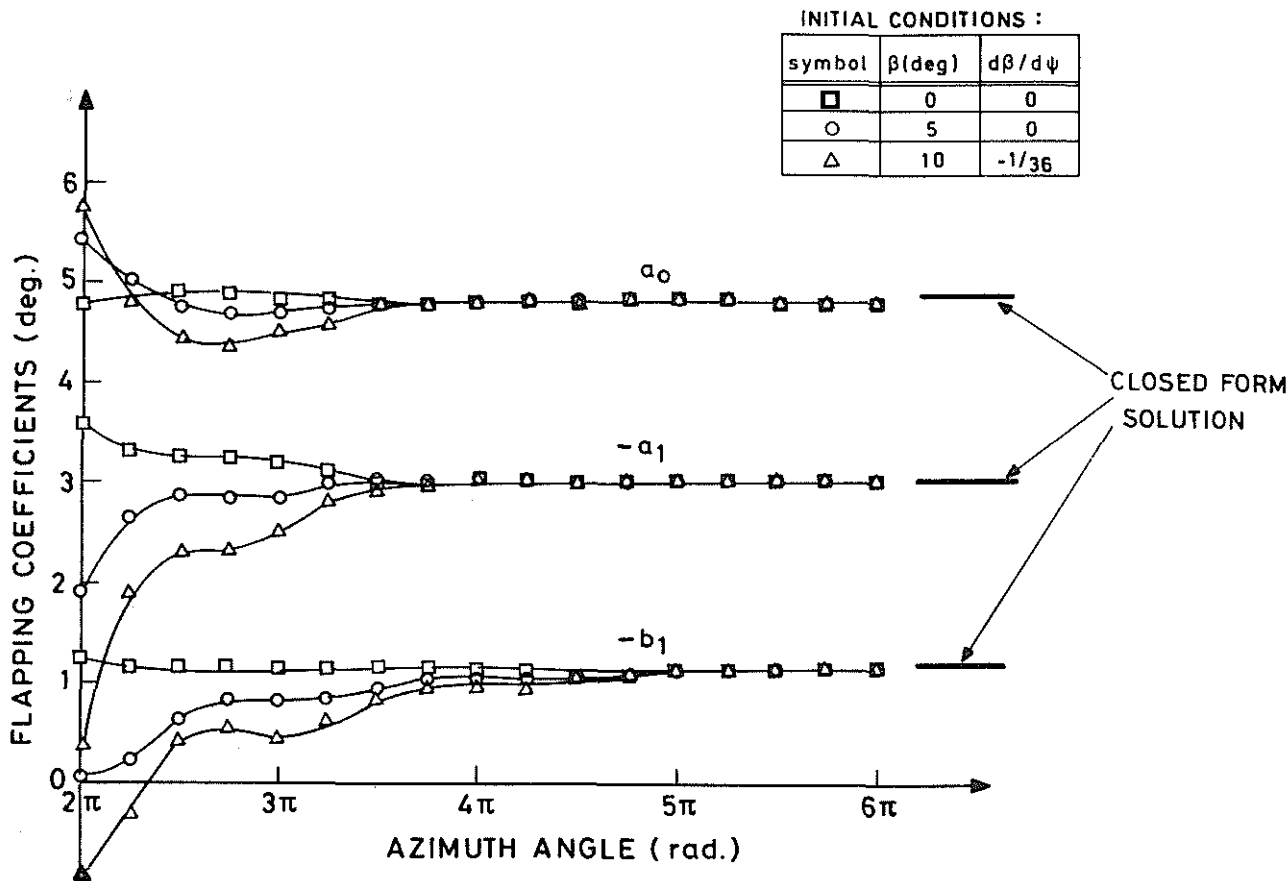


Fig. 5. Fourier analysis of the results of a simple case of uniform inflow.

significantly (after dynamic analysis) or if the value of  $v_{iav}$  has not been converged. As a result of updating the aerodynamic model, new values of  $\lambda_0$  (as function of the spanwise and azimuthal locations) and its derivatives with respect to  $\theta_k$ , are obtained.

With these new values of  $\lambda_0$  the code returns to the structural/dynamic model and integration of the equations of motion is continued. This procedure (see Fig. 3) is repeated until convergence of the blade motions and aerodynamic loads is obtained.

The solution procedure which has been described above can be performed in a fully automatic mode. But it has been found that interactive mode of operation is preferable. In this interactive mode the operator follows the solution procedure and make decisions according to the results. These decisions include: what level of updating of the aerodynamic model will be used, stop the integration of the equations of motion before convergence and

update the aerodynamic model, what will be the input value of  $v_{iav}$  for the calculations of the matrix  $[C]$ , etc. More details about the interactive mode appear in the next section.

As indicated before, the solution procedure can be started either with the structural/dynamic model, or with the aerodynamic model. In the above description the case of starting with the structural/dynamic model has been presented. The solution procedure can also be started by assuming an initial periodic behaviour of the blade motions, and use these motions ( $A$ ,  $B$  and  $\tilde{U}$ ) to calculate the  $\lambda_0$  distribution. Then the solution procedure continues in the same way that has been described above.

The next section will present how the present model is used in different cases. The theoretical results will be compared with experimental results which appear in the literature.

### 3. Examples

#### 3.1 Example No. 1

In this example one of the experiments of [11] is investigated. In this experiment a rotor model was tested in a wind tunnel at different flow speeds. At each speed the shaft angle of attack was chosen such that it gave a disc angle of attack of approximately one degree. The collective was set to yield a constant value of the thrust, at all the speeds. The measurements included the blade flapping and rotor forces and moments.

When the present model is used in this case, only flapping (as root dynamics) is taken into account. Assuming that the blade is relatively stiff, elastic deformations are neglected. During the aerodynamic calculations the blade is divided into nine segments by the following cross sections

$$\alpha_j = \cos[8.653^\circ(10-j)] \quad j = 1,2\dots10. \quad (7)$$

One of the problematic parameters in rotor calculations is the disc sideward tilt ( $b_1$ , see Eq. (6)). It is well known that using the assumption of uniform induced velocity yields very poor predictions of  $b_1$  [10,12]. The importance of using a more sophisticated aerodynamic model is presented very clearly in Fig. 6. In this figure the variations of  $b_1$  along the iterative procedure, for advance ratio  $\mu=0.12$ , is presented.

At the beginning a uniform induced velocity,  $v_{iav}=0.034$ , is assumed. Integration of the equations of motion is carried out (the initial conditions are zero flapping and zero velocity) and after three revolutions the value of  $b_1$  converges to the simple solution of uniform inflow (see Fig. 6). At this stage a complete aerodynamic analysis is performed. A value of  $(\tilde{v}_{iav})_{in}=0.034$  is assumed at the beginning of the calculations, and at the end a value of  $(\tilde{v}_{iav})_{out}=0.051$  is obtained. This indicates that the convergence of the aerodynamic model has not been obtained. But working in

an interactive mode and knowing that the solution is still far from the correct result, another complete aerodynamic calculation is not performed. Instead, the results of the last aerodynamic calculations are used while integration of the equations of motion is continued. The integration is carried out for four more revolutions until convergence of the blade periodic response is obtained. At the end of the seventh revolution another complete aerodynamic calculation is performed. In this case  $(\tilde{v}_{iav})_{in}=0.042$  while  $(\tilde{v}_{iav})_{out}=0.046$  (the input value has been chosen as the average between the input and output values of the previous aerodynamic analysis). It is clear that the aerodynamic model approaches convergence. Using the new aerodynamic data, the integration of the equations of motion for three more revolutions is performed. At the end of the tenth revolution a simplified aerodynamic analysis is performed (first level) by updating only the vector  $\{d\}$  (in Fig. 6 this case is denoted AER. CHECK). This analysis yields again a value of  $(\tilde{v}_{iav})_{out}=0.046$ . In order to obtain convergence of the aerodynamic model, another complete aerodynamic analysis is performed. In this analysis a value of  $(\tilde{v}_{iav})_{in}=0.045$  is chosen while a value of  $(\tilde{v}_{iav})_{out}=0.045$  is obtained. This result indicates convergence of the aerodynamic model. With this converged model, integration along four additional revolutions has been carried out. At the end of the fourteenth revolution, after convergence of the dynamic response, a first level aerodynamics analysis is performed which shows that the very small changes in the blade dynamics do not affect the aerodynamic model.

The above description (and Fig. 6) presents a typical iterative procedure. It is clear that by using previous experience and better initial assumptions, the convergence procedure can be accelerated significantly and instead of fourteen revolutions, complete convergence can be achieved after less than five revolutions. The present example has been brought in order to show that the whole procedure has good convergence properties and previous experience is not necessary in order to achieve a converged solution. The behaviour has been presented with respect to  $b_1$  (which is the problematic variable) but usually the interactive procedure includes a follow-up of all the variables, or a group of the important ones.

The disc sideward tilt,  $b_1$ , as a function of the advance ratio  $\mu$  is presented in Fig. 7. While the simple uniform induced velocity model yields poor results, the results of the present model are in satisfactory agreement with the experimental results. The experimental results are presented with the possible experimental scatter due to measurement errors (according to [11]). One should also note the difference (in the experimental results) between the isolated and aft rotors, and also the unexpected lateral flapping at hovering.

In Fig. 8 the longitudinal disc inclination  $a_1$  (see Eq. (6)), as function of the advance ratio, is presented. The rotor drag coefficient  $C_H$  is presented in Fig. 9. In both cases nice agreement between the theoretical and experimental results is obtained. This agreement is not surprising since usually the calculations of the parameters which are associated with the

longitudinal plane do not present difficulties, even when simple aerodynamic models are used.

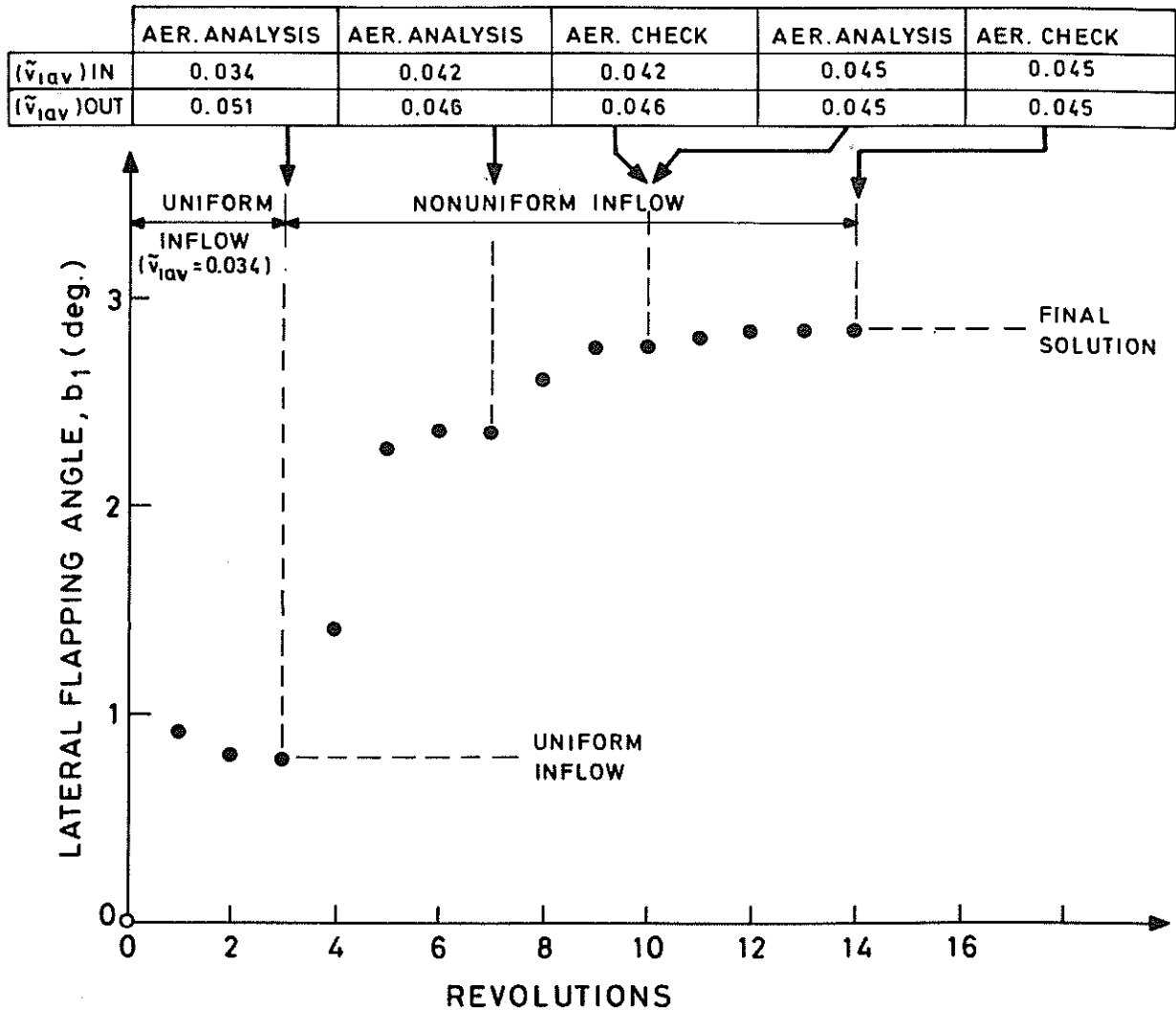


Fig. 6. Example 1 - Description of the Iterative Procedure.

A parameter where improved aerodynamic models are needed, in order to obtain satisfactory theoretical results, is the sideward force coefficient  $C_y$ . In Fig. 10  $C_y$  which is obtained by using the present analysis is compared with the experimental results. The theoretical results present a very good average to the scattered experimental results.

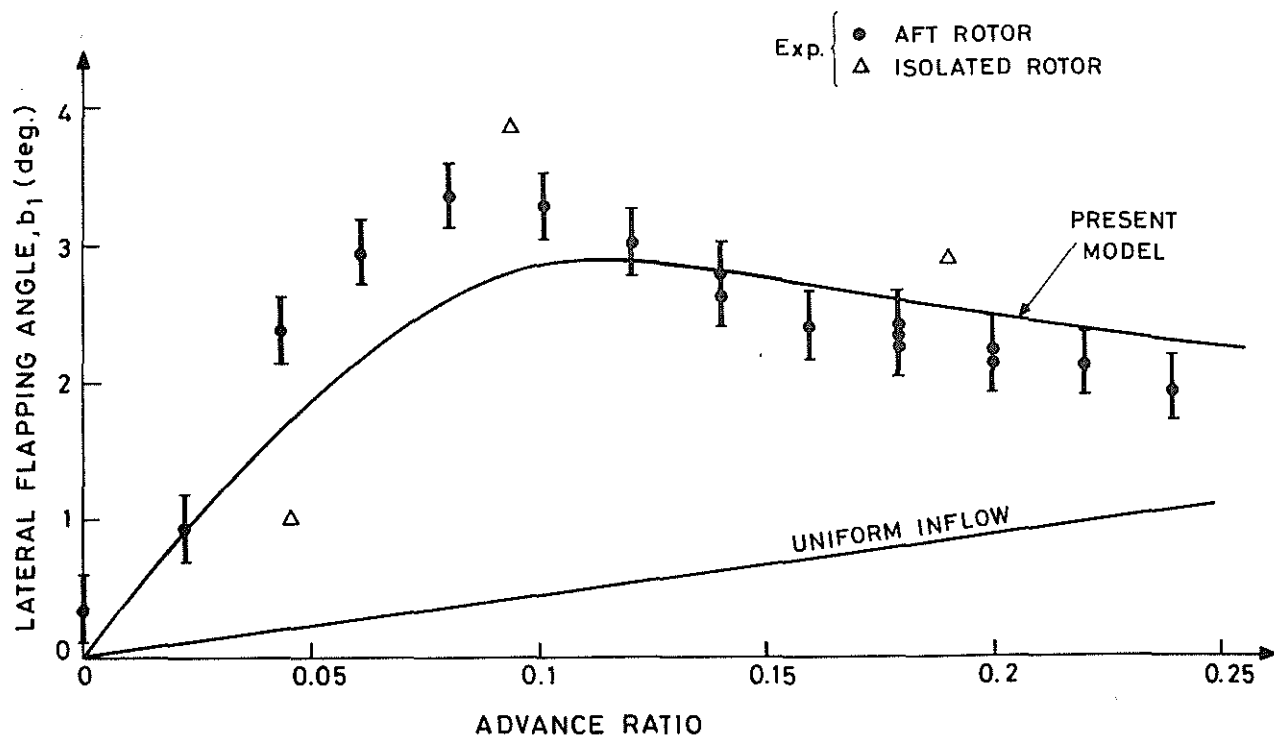


Fig. 7. Example 1 - The disc sideward tilt as function of the advance ratio.

### 3.2 Example No. 2

In this example calculations are performed for the case of the rotor of a H-34 Helicopter in forward flight. This is a fully articulated rotor having four blades with lead-lag dampers. The results are compared with experimental results from [13]. The flight condition is identical to the case which is described in Data Table No. 14 of [13]. The advance ratio in this case is 0.23. The shaft inclination, blade geometry, structural mass and aerodynamic properties are given in [13]. The pitch information of [13] is used as an input to the calculations. In a previous paper [2] the blade flapping and lead-lag motions were also used as an input when the aerodynamic loads were calculated. The results of [2] have indicated that the aerodynamic model give good results in this case. In the present example the flapping and lead-lag motions are obtained as an output of the complete aero-elastic analysis. Since flapping has been dealt with in the previous example, the lead-lag motion will be discussed here. The lead-lag angle  $\zeta$  (see Fig. 1) is

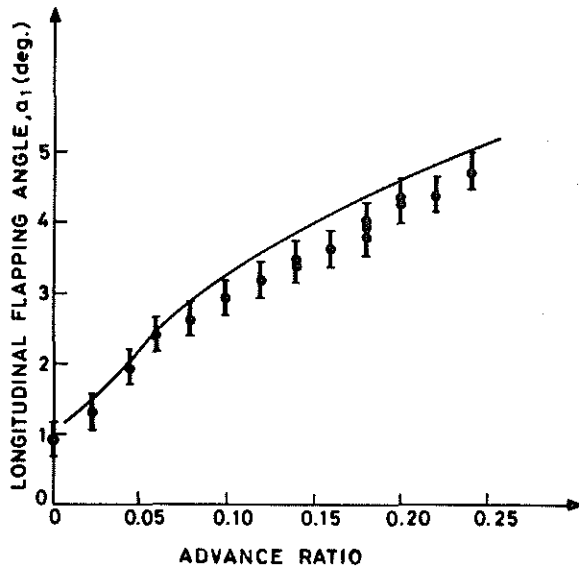


Fig. 8. Example 1 - The disc longitudinal flapping angle as function of the advance ratio.

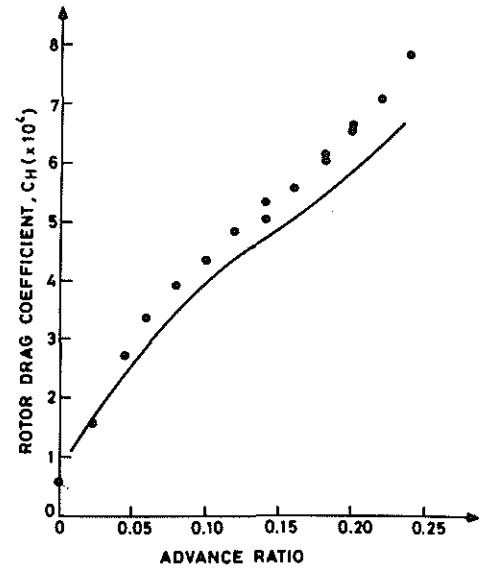


Fig. 9. Example 1 - The rotor drag coefficient as function of the advance ratio.

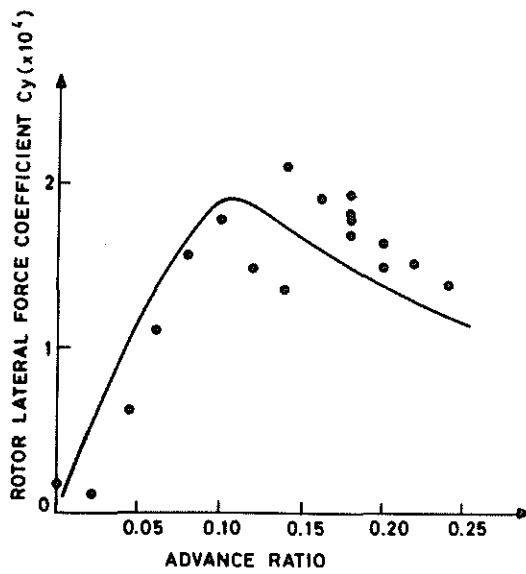


Fig. 10. Example 1 - The rotor lateral force coefficient as function of the advance ratio.

described as a Fourier series by the following equation:

$$\zeta = \sum_{n=0}^N (c_n \cos n\theta_k + d_n \sin n\theta_k) \quad (8)$$

In the next Table the results of the calculations are compared with the experimental results:

n	Theory		Experiment	
	c <sub>n</sub>	d <sub>n</sub>	c <sub>n</sub>	d <sub>n</sub>
0	-8.140	-	-7.140	-
1	0.320	-0.190	0.393	-0.071
2	-0.003	-0.026	-0.009	-0.024

Table - The first few harmonics of the lead-lag motion.

It is shown that the steady component is the most significant one while the others are much smaller. In both theory and experiment, the amplitude decreases as the harmonic number increases. It should be remembered that the lead-lag motion is very sensitive to the aerodynamic drag and lead-lag damper properties. Since the properties of both are not known in an accurate enough manner, it can be concluded that the agreement in the last table, between the experimental and theoretical results, is satisfactory.

In the present example, the elastic deformations along the blade are calculated too. The boundary conditions at the blade root are fairly complicated. Although the rotor is fully articulated both, the flapwise and chordwise root moments, are not zero in general. This fact is a result of the lead-lag damper and pitch angle at the root. Moreover, because of the cyclic rotations at the root, the flapwise and chordwise directions there (which are fixed relative to the blade) are changed in a periodic manner relative to the rotating hub directions. Therefore it seems that using the present technique of root dynamics is probably the only way of presenting the blade structural/dynamic behaviour in an accurate manner.

The shape functions in the series of  $\dot{v}$  and  $\dot{w}$  (the flapwise and chordwise displacements, respectively, see Eqs. (1a-b)) are the natural modes of

transverse vibrations of a clamped/free uniform non-rotating beam. Two terms in the series of  $v$  and three terms in series of  $w$  have been used. The shape functions in the series of  $\phi$  are the natural modes of torsional vibrations of a fixed/free beam. Two modes have been used in this series. Five terms are taken in the series of  $P$ , and are identical to those which have been described in [1]. The periodic behaviour of the coefficients is presented in Fig. 11. It can be seen that good convergence is obtained inside each of the

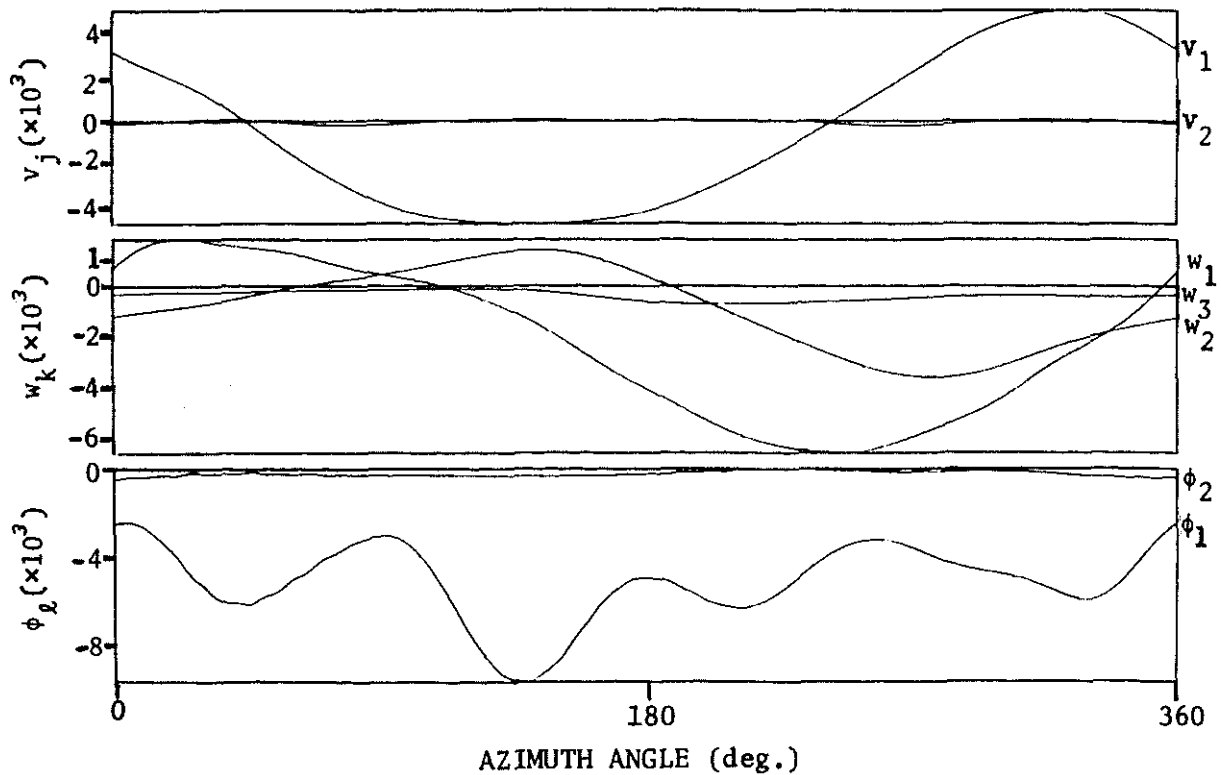


Fig. 11. Example 2 - The azimuthal variation of  $v_j, w_k, \phi_l$ .

series. It is also worth pointing out that it has been found that in this case, instead of solving the root and structural dynamics simultaneously, it is more efficient to solve them separately. At first the root dynamics is solved while the elastic deformations are considered as an input to the solution procedure. Then the structural deformations are calculated (integration with respect to time of the structural equations) while the root motions are considered as an input. This procedure is continued until convergence is obtained. It has been found that satisfactory convergence is usually obtained after only two solution cycles.

The blade deformations are used in order to calculate the components of the cross sectional resultant moment. In Fig. 12 the flapwise bending moment as function of the blade azimuthal location, at different cross sections

along the blade, is presented and compared with experimental results. Unlike other papers where the steady state was omitted here the comparison includes this component too. The agreement between theory and experiment is good in most of the cases. One should note the relatively very small flapwise moments which are obtained in the case of a fully articulated rotor (relative to the magnitude of the aerodynamic or inertia loads alone). These moments are very sensitive to the accuracy of presenting the boundary conditions at the root, the blade geometry and the exact distribution of the properties along the blades. Unfortunately these parameters are not fully defined in [13], while scatter in these parameters may cause different deviations.

The chordwise moment is presented in Fig. 13. Again if one recalls that this component depends to a large extent on the cross sectional aerodynamic drag and lead-lag damper, which are not defined in an accurate enough manner, it can be concluded that the agreement is satisfactory. Because there are usually problems with the steady-state component in strain-gauge measurements [13], the theoretical results were shifted such that their average value will match the average of the experimental results. This curve is also presented in Fig. 13 and exhibits a better agreement. The experimental results show a three per-revolution harmonic which is composed on the basic one per-revolution behaviour. This harmonic is not clearly obtained in the theoretical results.

The pitch horn load is presented in Fig. 14. This load is a direct result of the torsional moment at the blade root. This torsional component at the root, and along the blade, is very small compared with the other two components of the resultant moment. Therefore, it is expected that because of measuring problems relatively large deviations will appear in this case. Moreover, the torsional moment is very sensitive to small shifts of the cross sectional aerodynamic center and center of mass locations. Such small shifts probably exist but they are not measured. Therefore it has been assumed that the elastic axis, aerodynamic axis and center of mass axis are straight lines that always coincide. The average of the theoretical predictions of the pitch-horn load match very nicely the average of the experimental results.

#### 4. Conclusions

An accurate model of the aeroelastic behaviour of rotor blades in forward flight has been presented. This model is a combination of previously developed structural/dynamic model of helicopter blades, and a prescribed wake unsteady aerodynamic model of helicopter rotor in forward flight.

A special technique of combining these two sub-models and arriving at the steady-state periodic solution, has been described and successfully applied to solve different problems. It seems that the technique is consistent and ensures convergence without the need of significant background experience in its use. On the other hand, because of the interactive nature of the technique, experience can help in accelerating the convergence rate to a steady-state periodic solution.

The theoretical results have been compared with experimental results of two different experiments. Good agreement is obtained in most of the cases.

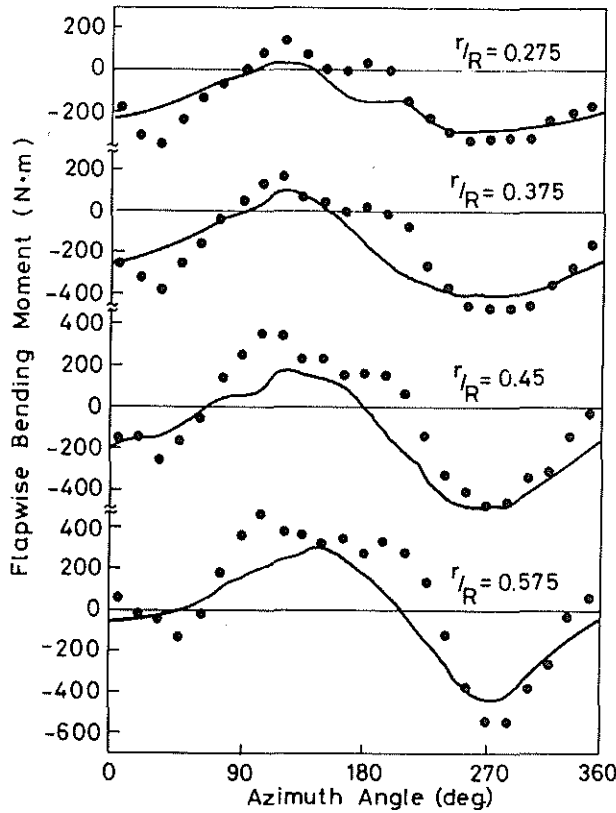


Fig. 12. Example 2 - The azimuthal variation of the flapwise bending moment.

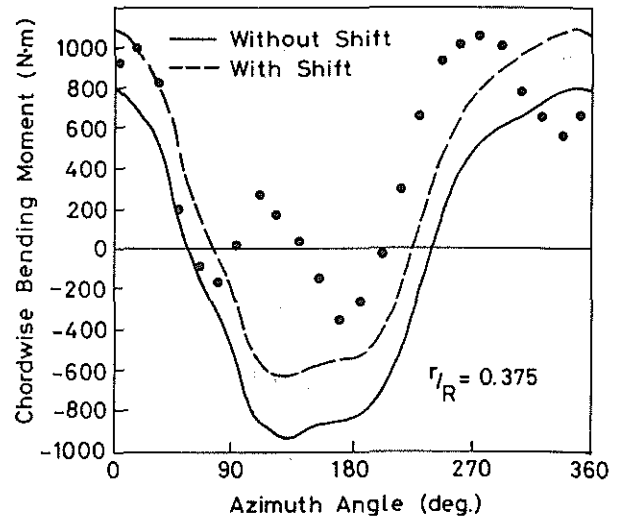


Fig. 13. Example 2 - The azimuthal variation of the chordwise bending moment.

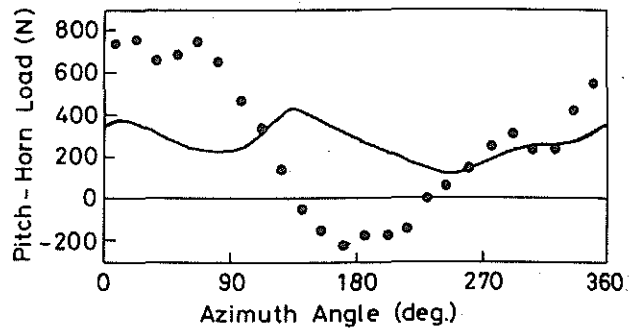


Fig. 14. Example 2 - The azimuthal variation of the pitch-horn load.

The model which has been presented here seems to be a very useful tool in calculating the aeroelastic response and loads of helicopter blades in forward flight. It is a relatively accurate model compared to other models which have been described in the literature, and makes possible the analysis of rotors which cannot be analysed by most of the other models (for example curved blades). It is planned to use the model in the near future in order to check the influence of different parameters on the aeroelastic response of helicopter blades.

#### Acknowledgement

The authors would like to thank Mrs. A. Goodman-Pinto for typing the paper, and Mrs. E. Nitzan and Mrs. R. Puvlic for the preparation of the figures.

## References

- 1) A. Rosen and O. Rand, A General Model of Helicopter Blade Dynamics, has been accepted for publication in Vertica (also proceedings of the Ninth European Rotorcraft Forum, Sept. 1983).
- 2) O. Rand and A. Rosen, A New Unsteady Prescribed Wake Model of the Aerodynamic Behavior of a Rotor in Forward Flight, Proceedings of the 26th Israel Annual Conference on Aviation and Astronautics, Feb. 1984, pp. 8-21.
- 3) P. Friedmann, Formulation and Solution of Rotary Wing Aeroelastic Stability and Response Problems, Vertica, Vol. 7, No. 2, 1983, pp. 101-142.
- 4) W. Johnson, Development of a Comprehensive Analysis for Rotorcraft - I. Rotor Model and Wake Analysis, Vertica, Vol. 5, 1981, pp. 99-129.
- 5) W. Johnson, Development of a Comprehensive Analysis for Rotorcraft - II Aircraft Model, Solution Procedure and Applications, Vertica, Vol. 5, 1981, pp. 185-216.
- 6) A. Rosen and O. Rand, A General Model of the Dynamics of Moving and Rotating Curved Rods, Department of Aeronautical Engineering, Technion - Israel Institute of Technology, TAE No. 514, Sept. 1983.
- 7) A. Rosen and O. Rand, Formulation of a Nonlinear Model for Curved Rods, Proceedings of the 26th Israel Annual Conference on Aviation and Astronautics, Feb. 1984, pp. 244-256.
- 8) A. Rosen and O. Rand, A General Model of the Dynamics of Moving and Rotating Rods, has been accepted for publication in Computers and Structures.
- 9) O. Rand and A. Rosen, Investigation of the Rotor Loads in Forward Flight Using an Unsteady Prescribed Wake Model, Part I - Derivation of the Model, Department of Aeronautical Engineering, Technion - Israel Institute of Technology, TAE NO. 513, June 1983.
- 10) A. Rosen and Z. Beigelman, The Influence of Different Inflow Models on the Coupled Flapping and Torsion of Helicopter Rotor Blades, Proceedings of the Eighth European Rotorcraft Forum, August 1982, Paper No. 3-10.
- 11) F.D. Harris, Articulated Rotor Blade Flapping Motion at Low Advance Ratio, J. American Helicopter Society, Vol. 17, No. 1, 1972, pp. 41-48.
- 12) W. Johnson, Comparison of Calculated and Measured Helicopter Rotor Lateral Flapping Angles, J. American Helicopter Society, Vol. 26, No. 2, 1981, pp. 46-50.
- 13) J. Scheiman, A Tabulation of Helicopter Rotor-Blade Differential Pressures, Stresses, and Motions as Measures in Flight, NASA TM X-952, March 1964.